Direct simulation of a jet diffusion flame

By B. J. Boersma

1. Motivation and objective

The main energy source in the Western world is the combustion of fossil fuels, and it will remain to be the major energy source for at least several decades to come. Everybody is aware of the problems connected to the combustion of these fuels. First, their supply is finite, and this means that they should be used economically. Second, during combustion of fossil fuels, air pollution is generated, e.g., in the form of toxic gases such as NO_x or SO_2 but also in the form of gases harmless for man such as CO_2, which are nevertheless considered harmful because they may influence our climate by processes such as the greenhouse effect. In view of these problems, it will be clear that combustion of fossil fuels with an optimal fuel efficiency and with a minimal production of pollutants must have a high priority.

The process of combustion is highly complex. It involves fluid mechanical processes such as turbulent mixing and heat transfer but also other processes such as radiation and chemistry. The fact that the combustion involves these very different processes makes it not only a highly multidisciplinary topic for research, but also a highly challenging one. For this reason the scientific problem of combustion has been nominated as one of the "Grand Challenges"to be solved when a Tera-flops computer becomes available, and this is the background of the project that we propose here.

In this project we aim to perform a numerical simulation of a non-premixed turbulent diffusion flame. The objective is to shed light on one of the important processes in combustion that have been mentioned above, namely turbulent mixing, which is an essential link in the modeling of combustion. In the past researchers and designers have used so-called Reynolds-averaged turbulence models to predict the combustion in various appliances. However, these models have their weaknesses, especially in the complicated environment of a flame, and they have, in general, failed to produce acceptable results. A factor contributing to this failure has been the fact that it is very difficult to perform measurements in the hostile environment of a combustion flame, and such measurements are needed for validating and developing turbulence models. Therefore, the problem of turbulent mixing within the combustion process is to be considered as unsolved.

Recently, new methods have become available for combustion research as a result of increasing computer power (especially due to the appearance of parallel computers). Two very powerful new methods are direct numerical simulation (DNS) and large eddy simulation (LES). The first technique (DNS) solves the governing equations for the combustion without any model. In the second method, a model is used for the small scales of motion. The first method is computationally very expensive but gives in general very reliable results. The second method (LES) is

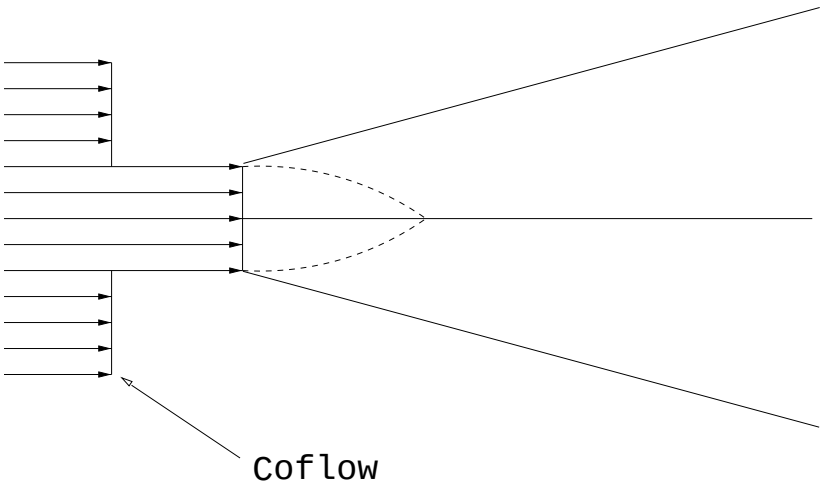

FIGURE 1. The geometry of the coflowing jet.

much cheaper, but the modeling of the small scales introduces an error. In this paper we will use DNS; there is also LES and experimental work going on for the same problem (see e.g. Steiner, and Su this volume).

1.2 The geometry

In Fig. 1 we show the geometry of the problem. The jet fluid (in general fuel) is injected in a slower flowing air (oxidizer) stream. In the experiment the Reynolds number based on the jet fluid is approximately between $5,000$ and $50,000$. The coflow velocity is typically 1 to 5% of the jet velocity.

For the DNS we will use a very simple binary reaction:

$$[Fuel] + [Oxidizer] \rightarrow 2[Prod]$$

The factor 2 is included to conserve mole fractions. The reaction rate of this reaction is given by

$$\dot{\omega} = Da \rho Y_f \rho Y_o \exp[-\hat{\Theta}]. \tag{1}$$

In which Da is the Dahmköhler number, ρ is the density, Y_f the fuel mass fraction, Y_o the oxidizer mass fraction, and

$$\hat{\Theta} = \beta \frac{1-\theta}{1-\alpha(1-\theta)}. \tag{2}$$

In which α is the heat release parameter and β the Zeldovich number. The non dimensional temperature θ is defined as $\theta = (T - T_o)/(T_a - T_o)$ with T_a as adiabatic flame temperature and T_o as room temperature.

2. Low Mach number approximation

There are basically two ways to compute chemically reacting flows with significant heat-release. The first option is to use a fully compressible flow solver (including acoustic waves). The second one is to use an incompressible solver with variable

density. The second method is very attractive for flows with low Mach numbers because numerical time steps are not related to the speed of sound. Furthermore, the formulation of the boundary conditions is much simpler than in the fully compressible case.

The low Mach number approximation of the equations of motion can be found in the literature (see e.g. Williams 1985) For completeness we will give the non-dimensional governing equations here. Conservation of mass reads

$$\frac{\partial \rho}{\partial t} + \nabla \cdot (\rho \mathbf{u}) = 0, \tag{3}$$

where $\mathbf{u}$ is the fluids velocity vector. Conservation of momentum

$$\frac{\partial \rho \mathbf{u}}{\partial t} + \nabla \cdot (\rho \mathbf{u}\mathbf{u}) = -\nabla P + \frac{1}{Re} \nabla \cdot \frac{\mu}{\mu_0} (\nabla \mathbf{u} + (\nabla \mathbf{u})^T) \tag{4}$$

In which P is the pressure, Re the Reynolds number, and μ the dynamic viscosity. The energy or temperature equation reads:

$$\frac{\partial \rho T}{\partial t} + \nabla \cdot \rho \mathbf{u} T = \frac{1}{RePr} \nabla \cdot \frac{\mu}{\mu_0} \nabla T + 2\dot{\omega} \tag{5}$$

with Pr the Prandtl number. Furthermore, we have two equations for the chemical species, i.e. one for the fuel and oxidizer.

$$\frac{\partial \rho Y_i}{\partial t} + \nabla \cdot \rho \mathbf{u} Y_i = \frac{1}{ReSc} \nabla \cdot \frac{\mu}{\mu_0} \nabla Y_i - \dot{\omega} \tag{6}$$

with Sc the Schmidt number. The equation of state gives a relation between density and temperature:

$$P = \rho T \tag{7}$$

For the temperature dependent viscosity μ we will use the following relation

$$\frac{\mu}{\mu_0} = \left(\frac{T}{T_0} \right)^{3/4} \tag{8}$$

The main assumption in the low Mach number approximation is that the pressure P can be written as:

$$P = P_0(t) + \gamma Ma^2 P_1 \tag{9}$$

In which $P_0(t)$ is the total pressure, which is only a function of time. For an open domain like our jet, the pressure $P_0(t)$ is a constant with an arbitrary value, say 1. This means that in the Navier-Stokes equations (4) P_1, which will be further on denoted by p, plays only a role and that $\rho T = 1$ at the lowest order.

3. Numerical method and parallel implementation

In this section we will give an outline of the numerical method which will be used to solve the governing equations. The spatial terms in the continuity and momentum equations are discretized with help of a second-order finite volume method on a staggered three-dimensional spherical grid (see e.g. Boersma *et al.* 1998). The convective term in the transport equations are treated with a TVD scheme (see e.g. Vreugdenhil and Koren 1993) to keep the scalar concentrations between the specified minimum and maximum, say 0 and 1. For this, we had to recast the transport equations in the following form:

$$\frac{\partial T}{\partial t} + \nabla \cdot \mathbf{u}T - T\nabla \cdot \mathbf{u} = \frac{1}{\rho}\frac{1}{PrRe}\nabla \cdot \frac{\mu}{\mu_0}\nabla T + \frac{2}{\rho}\dot{\omega} \tag{10}$$

The diffusive part of the transport equations is treated in a similar way as in the momentum equations.

The time advancement is accomplished with a predictor-corrector method similar to the one used by Najm, Wyckoff and Knio (1998). First the transport equations are integrated from time level n with an explicit Adams-Bashforth step to an intermediate level, i.e.

$$T^* - T^n = \Delta t[\frac{3}{2}(-A_t + D_t)^n - \frac{1}{2}(-A_t + D_t)^{n-1}] \tag{11}$$

where A_t and D_t stand for the advective and diffusive terms in the transport equations (equations for Y_i are similar). The equation of state, $P = \rho T$, is then used to find the density at the intermediate level. Also the momentum equations are integrated to the intermediate level,

$$\frac{\rho^* u^* - \rho^n u^n}{\Delta t} = [\frac{3}{2}(-A_m + D_m)^n - \frac{1}{2}(-A_m + D_m)^{n-1}] \tag{12}$$

In which A_m and D_m stand for the advective and diffusive terms in the momentum equations. The intermediate hydrodynamic pressure is determined from the pressure Poisson equation

$$\nabla^2 p^* = \frac{1}{\Delta t}[\nabla \cdot (\rho^* \mathbf{u}^*) + \frac{\partial \rho^*}{\partial t}] \tag{13}$$

The derivative $\partial\rho^*/\partial t$ is calculated with help of a backward difference formula using ρ^*, ρ^n and ρ^{n-1}. Once the Poisson equation is solved, $\rho^*\mathbf{u}^*$ can be corrected in the following way

$$\rho^*\mathbf{u}^* := \rho^*\mathbf{u}^* - \Delta t \nabla p^* \tag{14}$$

The next step is to use the Adams-Moulton corrector for the transport equations:

$$T^{n+1} - T^n = \frac{1}{2}[(-A_t + D_t)^n + (-A_t + D_t)^*]. \tag{15}$$

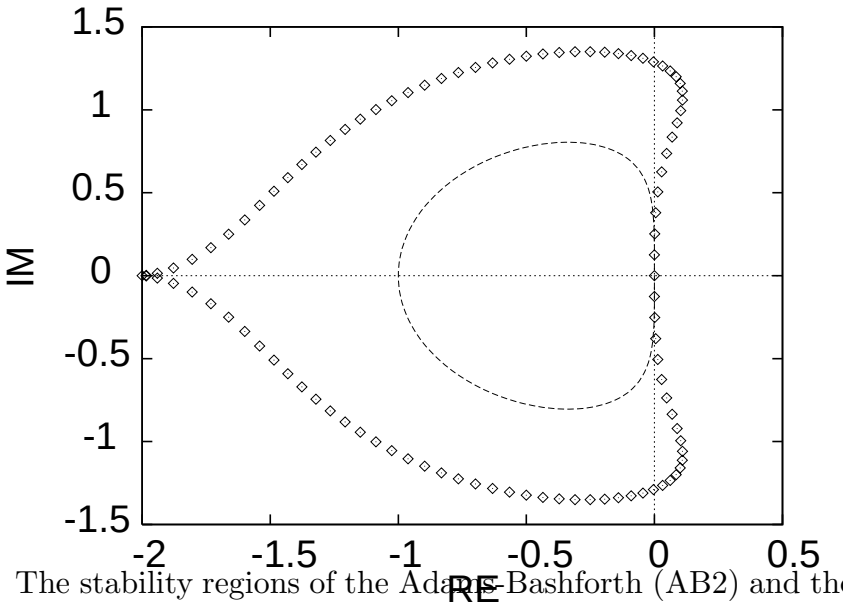

FIGURE 2. The stability regions of the Adams-Bashforth (AB2) and the predictor corrector (P-C) method. AB2: ---- ; P-C: ◇ .

The equation of state again gives the density, but now at time level $n+1$ Again the momentum equations are integrated:

$$\frac{\rho'\mathbf{u}' - \rho^n\mathbf{u}^n}{\Delta t} = \frac{1}{2}[(-A_m + D_m)^n + (-A_m + D_m)^*] \tag{16}$$

The Poisson equation is used to obtain the pressure at $n+1$, and the velocity correction gives the final velocity (or flux) at $n+1$.

The scheme above is quite similar to the one used by Rutland (1989) and the one used by Najm *et al.* (1998). In Rutland's work the predictor corrector method is replaced by a fully implicit method using Crank-Nicolson. The advantage of this method is that there is no restriction on the time step. However, for a full three-dimensional calculation, the solution of the matrix vector equation is very expensive. Najm *et al.* (1998) use the predictor-corrector strategy only for the transport equations (5), (6) and not for the full system of equations (4), (5) and (6). In Fig. 2 we show the stability regions of the method proposed by Najm *et al.* (1998) and of our method. It is clear that the full predictor corrector method has a considerably bigger time step without much extra work. Furthermore, the predictor-corrector scheme does not have the weak instability for advection which the second-order Adams-Bashforth method has.

3.1 Boundary conditions

In this section we will describe the boundary conditions for the coflowing jet calculations. At the inflow all components of the velocity are prescribed on the staggered grid:

$$u_r = U\cos\theta \tag{17}$$

$$u_\theta = -U\sin\theta \tag{18}$$

$$u_\phi = 0 \tag{19}$$

$$T = 1,\ Y_f = 1,\ Y_o = 0, \quad \text{In the orifice}$$

$$T = 1,\ Y_f = 0,\ Y_o = 1, \quad \text{In the coflow}$$

where U is the velocity (jet or coflow) in a Cartesian system. This boundary condition will be used for both the velocity and predicted velocity ($\mathbf{u}^*$).

At the lateral boundary of the jet, several boundary conditions can be used, for instance, the frequently used free-slip conditions (Gresho 1991) which read:

$$u_\theta = \frac{\partial u_r}{\partial \theta} = \frac{\partial u_\phi}{\partial \theta} = 0. \tag{20}$$

With this boundary condition no entrainment of fluid into the jet is possible because u_θ is set equal to zero. Another possible boundary condition is the so-called traction free boundary condition, i.e. the traction of the stress tensor with the unit normal on the boundary, Gresho (1991)

$$(-p\delta_{ij} + \tau_{ij}) \cdot n_\theta = 0, \tag{21}$$

For simplicity we will assume that the pressure p at the lateral boundary is constant. Without loss of generality we can also assume that the pressure at this boundary is zero. In the computational domain the pressure is calculated by the model, and the pressure difference between the pressure at the border and the pressure in the computational domain will determine the entrainment of fluid in or out of the jet.

At the outflow boundary we apply a convective boundary condition (see e.g. Akselvoll and Moin 1996).

$$\frac{\partial \rho \mathbf{u}}{\partial t} = -U \frac{\partial \rho \mathbf{u}}{\partial r} \tag{22}$$

where $U = U(\theta)$ is the mean velocity at the outflow boundary. This boundary condition is applied to the predicted velocity $\mathbf{u}^*$. The convective boundary conditions are discretized using a first-order upwind method in space and a first order discretization in time.

From numerical experiments, we found that the flow is rather sensitive to the convective outflow velocity U. It turns out that errors in the outflow boundary condition generate rather high pressure gradients near this boundary, and this influences the entrainment over the lateral boundary, which changes the total behavior of the jet. These large pressure gradients can be avoided by enforcing that the integral,

$$\int\int\int (\frac{\partial \rho^*}{\partial t} + \nabla \cdot \rho \mathbf{u}^*) dVol = \int\int\int \frac{\partial \rho^*}{\partial t} dVol + \int\int \rho \mathbf{u}^* dS, \tag{23}$$

is exactly zero. We enforce this by chancing $\rho \mathbf{u}_*$ at the outflow boundary.

3.2 Parallel implementation

The numerical method outlined above has been implemented on parallel machines using the message passing interface (MPI). Let N_r, N_θ and N_ϕ be the number of grid points in the coordinate directions and N_p the number of processors. It is clear that from a physical point of view N_r will be larger than N_θ and N_ϕ. Therefore, we have decided to distribute the radial direction over the CPU's. Thus on every CPU there are $N_r/N_p \times N_\theta \times N_\phi$ points. To minimize the communication we have added two ghost points in the radial direction, so actually there are $(N_r/Np+2) \times N_\theta \times N_\phi$ point on every CPU. With these ghost points all the explicit updates can be carried out without communication.

The Poisson equation is solved with a combination of Fast Fourier and Cyclic-reduction methods (see e.g. Boersma *et al. 1998*). The Fast Fourier transform of the right-hand side of the Poisson equation in the ϕ direction is local (no communication). The results of Fourier Transform are then redistributed to a distribution $N_r \times N_\theta \times N_\phi/N_p$. The two-dimensional (Helmholtz) problems in r and θ can be solved efficiently with the **BLKTRI** routine from the public domain package **FISHPAK**. The solutions of the Helmholtz problems are again redistributed to the $N_r/N_p \times N_\theta \times N_\phi$ distribution, and another local Fast Fourier Transformation gives the pressure in physical space.

The parallel strategy outlined above scales very well as can be seen from Table 1.

Table 1. Scalability of the parallel code

N_p	Grid	CPU/Δt
4	128^3	62.1 sec
8	128^3	31.2 sec
16	128^3	16.1 sec
32	128^3	8.6 sec
64	128^3	5.1 sec

4. Results

To validate the parallel code we performed a calculation of a cold coflowing jet with a Reynolds number based on the diameter of $4,000$ and a velocity excess of 10. The important parameters for this simulation are listed in Table 2.

Table 2. Some important parameters for the cold jet.

$N_r \times N_\theta \times N_\phi$	$768 \times 128 \times 96$
L_r	45 D
N_p	48
Re_d	4,000
λ	10

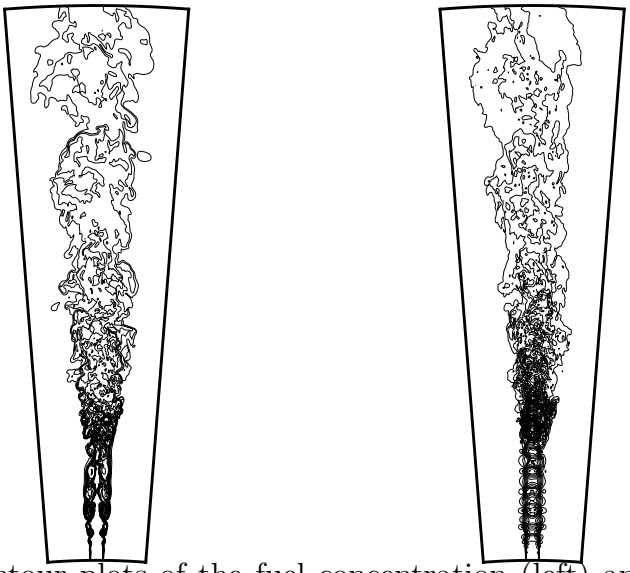

FIGURE 3. Contour plots of the fuel concentration (left) and the axial velocity (right) in the cold jet.

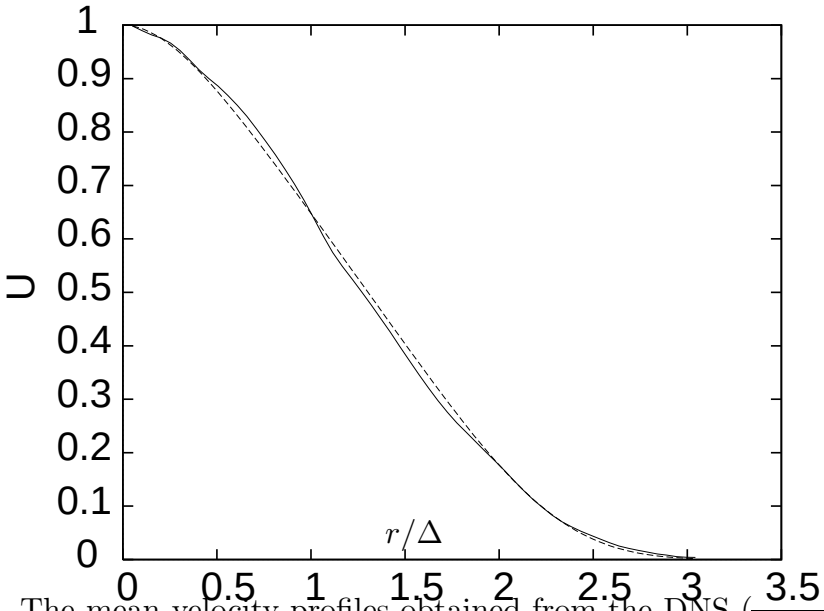

FIGURE 4. The mean velocity profiles obtained from the DNS (———) and from the experiment of Nickels and Perry, 1996 (- - - -).

In Fig. 3 we show a contour plot of the distribution of the scalar field in the cold jet. Close to the jet orifice an axisymmetric Kelvin-Helmholtz instability is present. Further downstream these structures break up in fully three-dimensional ones. In Fig. 4. we show that the mean self-similar velocity profile obtained from the DNS and also the curve fit through the experimental data of Nickels and Perry (1996). It should be noted that the profiles are scaled with the width Δ and not with the

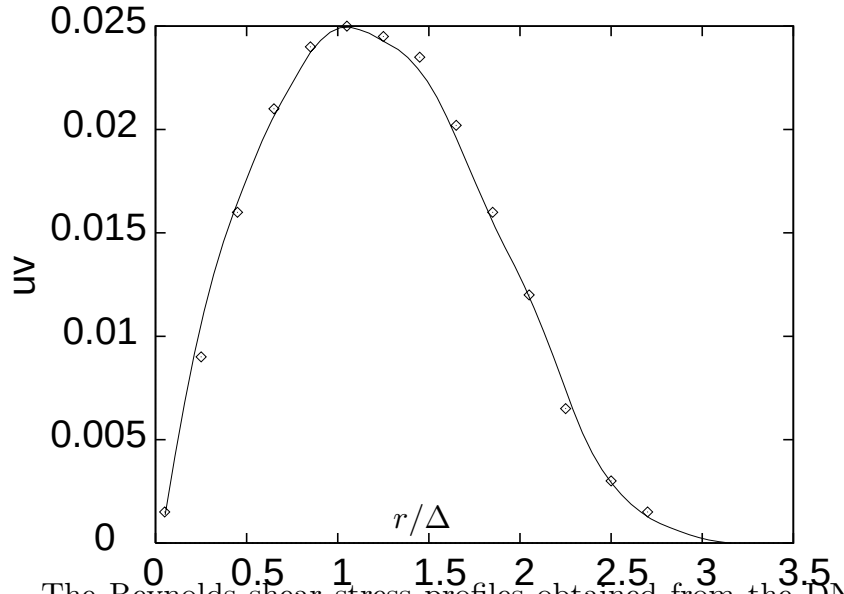

FIGURE 5. The Reynolds shear stress profiles obtained from the DNS (———) and from the experiment of Nickels and Perry, 1996 (- - - -).

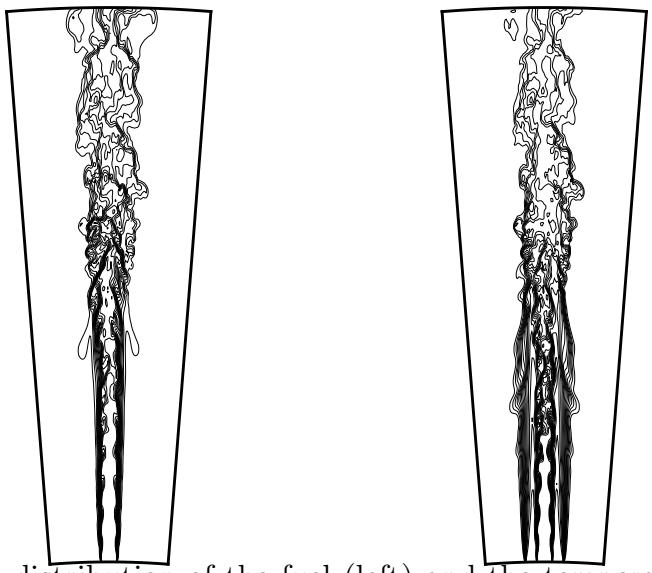

FIGURE 6. The distribution of the fuel (left) and the temperature (right) in the hot jet.

distance to the virtual origin. The agreement between experiment and simulation is rather good. This can also be seen from Fig. 5 in which we compare the computed Reynolds stress (DNS) with the experimental data of Nickels and Perry (1996).

Finally, we show some qualitative pictures of a heated jet. The jet geometry shown in Fig. 1 together with the assumed chemistry might lead to a lifted flame, which requires a very long domain. At this stage we do not want to do a calculation for such a flame because it requires a huge amount of CPU time. Therefore, we have chosen a jet with a pilot, which keeps the flame attached to the orifice. The fluid

leaving the pilot has a temperature of $0.99T_a$ and corresponding fuel and oxidizer concentrations. The effect of the pilot on the flow itself will be small because it has a very small momentum flux compared to the jet (approximately 5%). Figure 6 shows a contour plot of the concentration of fuel. It is clear that the combined effect of temperature/density variation plus increased viscosity due to higher temperature strongly suppresses the Kelvin-Helmholtz instability, leading to an almost laminar flow close to the jet orifice. (The high temperature in the initial shear layer increases the viscosity by more than a factor of three.) Further downstream there is still a clear transition to a fully turbulent state. Figure 6 (right) shows the density in the jet. Here we see more or less the same behavior as in Fig. 6 (left).

5. Conclusions and future work

We have shown that the developed numerical method is capable of simulating cold coflowing jets quite accurately. This gives us confidence for the heated case in which there is hardly any reliable experimental data available. From the preliminary results for the heated jet, it is clear that the combined effect of density variation and increased viscosity has a strong damping influence on the Kelvin-Helmholtz instability, leading to a delayed transition and a flow with considerably less small scales. Therefore, in future calculations it is probably possible to increase the Reynolds number and still resolve all scales of motion for the hot jet. In the near future the results of the DNS will be compared with the LES data obtained for the same geometry by Steiner (this volume) and with the experimental data obtained by Su (this volume).

REFERENCES

Akselvoll, K., & Moin, P. 1996 Large-eddy simulation of turbulent confined coannular jets. *J. Fluid Mech.* **315,** 387.

Boersma, B. J., Brethouwer, G., & Nieuwstadt, F. T. M. 1998 A numerical investigation on the effect of the inflow conditions on the self-similar region of a round jet. *Phys. Fluids.* **10,** 899-909.

Gresho, P. M. 1991 Incompressible fluid dynamics: Some fundamental formulation issues. *Ann. Rev. Fluid Mech.* **23,** 413-454.

Najm, H. N., Wyckoff, P. S., & Knio, O. M. 1998 A semi-implicit numerical scheme for reacting flow. *J. Comp. Phys.* **143,** 381-402.

Nickels, T. B. & Perry, A. E. 1996 An experimental and theoretical study of the turbulent coflowing jet. *J. Fluid Mech..* **309,** 157-183.

Rutland, C. J. 1989 Effects of strain, vorticity, and turbulence on premixed flames. *Report TF-44,* Stanford CA.

Williams, F.A. 1985 Combustion Theory,Addison-Wesley, New-York.

Vreugenhil, C. B., & Koren, B., 1993 Numerical Methods for Advection-Diffusion Problems. *Notes on Numerical Fluid Mechanics.* **45,** Vieweg, Braunschweig.